Pflügers Archiv - European Journal of Physiology (2019) 471:1127–1142
https://doi.org/10.1007/s00424-019-02280-5

SIGNALING AND CELL PHYSIOLOGY

Ciliary beating amplitude controlled by intracellular Cl^- and a high rate of CO_2 production in ciliated human nasal epithelial cells

Taka-aki Inui[1,2] · Kentaro Murakami[1,2] · Makoto Yasuda[2] · Shigeru Hirano[2] · Yukiko Ikeuchi[1,3] · Haruka Kogiso[1,3] · Shigekuni Hosogi[1] · Toshio Inui[3,4] · Yoshinori Marunaka[1,3,5] · Takashi Nakahari[3]

Received: 23 January 2019 / Revised: 25 April 2019 / Accepted: 29 April 2019 / Published online: 18 May 2019

Abstract

The ciliary transport is controlled by two parameters of the ciliary beating, frequency (CBF) and amplitude. In this study, we developed a novel method to measure both CBF and ciliary bend distance (CBD, an index of ciliary beating amplitude) in ciliated human nasal epithelial cells (cHNECs) in primary culture, which are prepared from patients contracting allergic rhinitis and chronic sinusitis. An application of Cl^--free NO_3^- solution or bumetanide (an inhibitor of $Na^+/K^+/2Cl^-$ cotransport), which decreases intracellular Cl^- concentration ($[Cl^-]_i$), increased CBD, not CBF, at 37 °C; however, it increased both CBD and CBF at 25 °C. Conversely, addition of Cl^- channel blockers (5-nitro-2-(3-phenylpropylamino) benzoic acid (NPPB) and 4-[[4-Oxo-2-thioxo-3-[3-trifluoromethyl]phenyl]-5-thiazolidinylidene]methyl] benzoic acid (CFTR(inh)-172)), which increase $[Cl^-]_i$, decreased both CBD and CBF, suggesting that CFTR plays a crucial role for maintaining $[Cl^-]_i$ in these cells. We speculate that Cl^- modulates activities of the molecular motors regulating both CBD and CBF in cHNECs. Moreover, application of the CO_2/HCO_3^--free solution did not change intracellular pH (pH_i), and addition of an inhibitor of carbonic anhydrase (acetazolamide) sustained pH_i increase induced by the NH_4^+ pulse, which transiently increased pH_i in the absence of acetazolamide. These results indicate that the cHNEC produces a large amount of CO_2, which maintains a constant pH_i even under the CO_2/HCO_3^--free condition.

Keywords Airway · Intracellular Cl^- · Intracellular pH · NH_4^+ pulse · Ciliated human nasal epithelial cell

✉ Makoto Yasuda
myasu@koto.kpu-m.ac.jp

✉ Takashi Nakahari
nakahari@fc.ritsumei.ac.jp

[1] Department of Molecular Cell Physiology, Graduate School of Medical Sciences, Kyoto Prefectural University of Medine, Kyoto 602-8566, Japan

[2] Department of Otolaryngology-Head and Neck Surgery, Graduate School of Medical Science, Kyoto Prefectural University of Medicine, Kyoto 602-8566, Japan

[3] Research Laboratory for Epithelial Physiology, Research Organization of Science and Technology BKC, Ritsumeikan University, Kusatsu 525-8577, Japan

[4] Saisei Mirai Clinics, Moriguchi 570-0012, Japan

[5] Research Institute for Clinical Physiology, Kyoto Industrial Health Association, Kyoto 604-8472, Japan

Introduction

Nasal mucociliary clearance consists of the surface mucous layer and the beating cilia lining the nasal mucosa [1, 28, 37]. Inhaled small particles trapped by the surface mucous layer are swept from the nasal cavity by the beating cilia. The beating cilia play a key role in the maintenance of a healthy nasal cavity, since their impairment, such as primary ciliary dyskinesia, causes sinusitis [1, 28, 37]. Thus, the mucociliary clearance is compared to a belt conveyer system for removing inhaled small particles from the sinonasal and nasal cavities, in which beating cilia are the engine [1, 8, 28, 37].

In many studies, only ciliary beating frequency (CBF) has been measured to evaluate the activity of ciliary beating and little attention has been paid to the amplitude [8, 21, 22, 28, 30, 32, 36, 42]. Our previous studies demonstrated that activities of the ciliary beating are controlled by two parameters, i.e., the ciliary beat angle (CBA, an index of ciliary beat

amplitude) and CBF [13, 15–20]. Increases in both CBA and CBF have been shown to enhance the ciliary transport in the airway surface [16, 20]. However, the measurement of CBA has some difficulties, because it requires the fine video frame image of beating cilia with a high time and spatial resolution [20]. Recent development of the video-microscopy equipped with high-speed camera has enabled us to observe the fine movement of each cilium. In our previous studies, CBA was measured as an index of ciliary beating amplitude, using the side view of isolated airway ciliary cells [13, 15–20].

However, in a planar sheet of ciliated cells, such as ciliated human nasal epithelial cells (cHNECs) cultured on the filter, it is not easy to observe the beating cilia from the side, because, in the cell sheet, ciliated cells are observed from above. We developed a novel method using an image analysis program for measuring the amplitude of ciliary beating in the cell sheet of cHNECs [15, 16]. The program calculates the light intensity change of a line set on the video image of a beating cilium and reports the time course of light intensity change. The reported image shows the amplitude of ciliary beating [15, 16, 39]. We measured the amplitude as ciliary beat distance (CBD, an index of ciliary beat amplitude), using the reported images.

Previous studies suggest that a decrease in intracellular Cl^- concentration ($[Cl^-]_i$) coupled with cell shrinkage modulates the airway ciliary beating [14–16, 30, 36]. Our recent studies revealed that an activation of Cl^- channels leading to a decrease in $[Cl^-]_i$ enhances the amplitude of airway ciliary beating [3, 13, 15, 16]. In this study, we measured CBD and CBF in the cHNEC cell sheet, upon decreasing $[Cl^-]_i$. The aim of this study is to confirm the effects of a low $[Cl^-]_i$ on CBD and CBF in cHNECs, using this novel method.

Materials and methods

Ethical approval

This study is approved by the ethics committee of the Kyoto Prefectural University of Medicine (RBMR-C-1249-4) and Ritsumeikan University (BKC-HM-2018-022) and the informed consent obtained from patients prior to the surgery (RBMR-C-1249-4). Human nasal tissue samples (nasal polyp, uncinate process, or inferior turbinate) were resected from the patients requiring surgery for their chronic sinusitis or allergic rhinitis. The samples were immediately cooled in the control solution (4 °C) and kept until cell isolation. The cell isolation was performed within 3 h after resection.

Solution and chemicals

The CO_2/HCO_3^--containing control solution contained (in mM): NaCl, 121; KCl, 4.5; $NaHCO_3$, 25; $MgCl_2$, 1; $CaCl_2$, 1.5; Na-HEPES, 5; H-HEPES, 5; and glucose, 5. To prepare the CO_2/HCO_3^--free control solution, $NaHCO_3$ was replaced with NaCl, and to prepare the CO_2/HCO_3^--free and Cl^--free NO_3^- solution, Cl^- was replaced with NO_3^-. To prepare test solutions with various Cl^- concentrations, an appropriate amount of CO_2/HCO_3^--free and Cl^--free NO_3^- solution was added to the CO_2/HCO_3^--free control solution. To prepare EGTA-containing Ca^{2+}-free solution, $CaCl_2$ was removed from the CO_2/HCO_3^--containing control solution and EGTA (1 mM) was added. The CO_2/HCO_3^--containing solutions were aerated with 95% O_2 and 5% CO_2 and the CO_2/HCO_3^--free solutions were with 100% O_2. The pH of solutions was adjusted to 7.4 by adding 1 N-HCl or 1 N-HNO_3, as appropriate. The experiments were carried out at 37 °C. Because activities of the airway ciliary beating depend on temperature [8, 22, 42]. Heparin, elastase, bovine serum albumin (BSA), dimethyl sulfoxide (DMSO), penicillin, streptomycin, trypsin, and trypsin inhibitor were purchased from Wako Pure Chemical Industries, Ltd. (Osaka, Japan); DNase I, 5-nitro-2-(3-phenylpropylamino) benzoic acid (NPPB), 4-[[4-Oxo-2-thioxo-3-[3-trifluoromethyl]phenyl]-5- thiazolidinylidene]methyl] benzoic acid (CFTR(inh)-172), acetazolamide and amphotericin B were from Sigma Chemical Co. (St Louis, MO, USA); and N-ethoxycarbonylmethyl-6-methoxyquinolinium bromide (MQAE) was from Dojindo Laboratories. (Kumamoto, Japan). All reagents were dissolved in DMSO and prepared to their final concentrations immediately before the experiments. The DMSO concentration did not exceed 0.1%, and DMSO at this concentration has no effect on CBF and CBA [13–21, 30].

PneumaCult-Ex and PneumaCult-ALI basal culture medium for culturing of cHNEC at air liquid-interface (ALI) were purchased from STEMCELL Technology (Vancouver, BC, Canada) [24]. The complete PneumaCult-Ex Medium contained PneumaCult-Ex 50× Supplement (20 μl/ml), hydrocortisone (2.5 μl/ml), penicillin (100 unit/ml), and streptomycin (100 μg/ml) in the PneumaCult-Ex Basal Medium, and the complete PneumaCult-ALI Medium contained PneumaCult-ALI 10× Supplement (0.1 ml/ml), PneumaCult-ALI Maintenance Supplement (10 μl/ml), heparin (1 μl/ml), hydrocortisone (2.5 μl/ml), penicillin (100 unit/ml), and streptomycin (100 μg/ml) in PneumaCult-ALI Basal Medium.

Cell preparation

Each resected sample by the operation was treated with elastase to isolate cHNECs [13–21, 30, 35, 40, 41]. Briefly, the resected samples were incubated for 40 min at 37 °C in the CO_2/HCO_3^--containing control solution containing elastase (0.02 mg/ml), DNase I (0.02 mg/ml), and BSA (3%). Following this incubation, the samples were minced by fine forceps in the control solution containing DNase I (0.02 mg/ml) and BSA (3%). The cells were washed three times with centrifugation at 160×*g* for 5 min and then, they were sterilized by amphotericin B (0.25 μg/ml) in Hams's F-12 with L-Gln for 15 min. After centrifugation, the cells were plated in the collagen-coated flask

(Corning, 25 cm^2) with the complete PneumaCult-Ex Medium, which was changed every second day. The culture cells reached confluence within 10–14 days. Upon reaching confluence, the cells were washed with PBS (5 ml) and then, incubated with Hank's balanced salt solution (HBSS) (2 ml) containing 0.1 mM EGTA and 0.025% trypsin for 10 min at 37 °C. Then, a trypsin inhibitor (1 mg/ml) resolved in HBSS (2 ml) was added. The cell suspension was washed with centrifugation (160×*g* for 5 min). After washing, the cells were re-suspended in the complete PneumaCult-Ex Medium (6 ml) and counted the number of cells. Then, cells (1–2 × 10^6 cells/insert, 400 μl) were seeded on culture inserts (3470, 6.5-mm Transwell filter, Coastar Corporation), which were bathed in the complete PneumaCult-Ex Medium (500 μl) in the basal chamber. Upon reaching confluence (after 4–6 days), the medium of the apical side was removed and the medium of the basolateral side was replaced with the complete PneumaCult-ALI (Air Liquid Interface) Medium (ALI condition). The cells were cultured under the ALI condition for 3–4 weeks until they differentiated to cHNECs [16], and then, they were used for the experiments.

Measurements of CBD, CBA, and CBF

The permeable support filter with the cHNECs was cut into small pieces (squares of sides 2–5 mm). A cutted filter with cHNECs was placed on a coverslip precoated with Cell-Tak (Becton Dickinson Labware, Bedford, MA, USA), and was set in a micro-perfusion chamber (20 μl) mounted on an inverted light microscope (Eclipse Ti, Nikon, Tokyo, Japan) connected to a high-speed camera (FASTCAM-1024PCI, Photron Ltd., Tokyo, Japan). The stage of microscope was heated to 37 °C, since CBFs have been shown to depend on temperature [8, 16, 22, 42]. The cells were perfused at 200 μl/min with the CO_2/HCO_3^--containing control solution aerated with a gas mixture (95% O_2 and 5% CO_2) at 37 °C. The video images of cHNECs were recorded for 2 s at 500 fps [13, 15–21]. An image analysis program (DippMotion 2D, DITECT, Tokyo, Japan) was used to measure CBA, CBD, and CBF. The method to measure CBA and CBF has previously been reported in detail [20]. CBA was measured in the beating cilia that could be observed from the side (Fig. 1a, b); these cells were selected from the cHNECs on the filter, although most of the beating cilia are viewed from the top (Fig. 1c, d). The angle between the start and end of effective stroke was measured as CBA (Fig. 1b). The beating cilia viewed from the top were selected (Fig. 1c, d), and the distance between the start and end of an effective stroke was measured as CBD (Fig. 1c, e). The enhancement of ciliary beat amplitude increases CBA or CBD. When we set a line "A–B" on video images of a beating cilium (Fig. 2a2), the image analysis program reported the image showing the time course of the light intensity change along the line "A–B" (Fig. 2c). The reported image shows the waveform of beating cilium (Figs. 1e and 2c). The peak of the waveform, "line S" shows the start of effective stroke and the bottom, "line E" shows the end of effective stroke, and the distance from the peak to the bottom is the CBD ("←→" in Fig. 2c).

The ratios of CBA, CBF, and CBD to their baseline values were calculated (CBA_t/CBA_0, CBF_t/CBF_0, and CBD_t/CBD_0), where the subscript 0 or *t* indicates the time before or after the start of experiments, respectively. These ratios were used to compare these parameters among experiments. CBA_0, CBF_0, and CBD_0 were calculated as the averages of CBAs, CBFs, and CBDs measured every 1 min during control perfusion (5 min). Each experiment was carried out using 5–9 cover slips from three to six inserts. In each coverslip, we selected 1–3 cells and measured their CBFs and CBDs. The CBF and CBD ratios calculated from 5 to 12 cells were plotted in the figures and *n* shows the number of cells.

Measurements of $[Cl^-]_i$ and pH_i

Changes in $[Cl^-]_i$ were monitored by the fluorescence of a chloride-sensitive dye, MQAE (N-ethoxycarbonylmethyl-6-methoxyquinolinium bromide) [12–16, 27, 31]. The cHNECs in culture were incubated with an EGTA-containing Ca^{2+}-free solution for 10 min to isolate cHNECs from the filter. The isolated cHNECs were incubated with 10 mM MQAE for 45 min at 37 °C. MQAE was excited at 780 nm using a two-photon excitation laser system (MaiTai, Spectra-Physics, Santa Clara, CA, USA), and the emission was 510 nm. The ratio of fluorescence intensity (F_0/F_t) was used as an index of $[Cl^-]_i$ [13–16, 27, 31]. The subscript 0 or *t* shows the time before or after the start of experiments, respectively.

To measure intracellular pH (pH_i) of cHNECs, we used carboxy-SNARF-1 (a pH-sensitive fluorescent dye) [12, 15, 16]. Cells isolated from the filter were incubated with carboxySNARF1-AM (10 μM, Spiro[7H-benzo[c]xanthene-7,1′(3H)-isobenzofuran]-ar′-carboxylic acid, 3-(acetyloxy)-10-(dimethylamino)-3′-oxo-, (acetyloxy)methyl ester) for 45 min at 37 °C and the cells were set in the chamber mounted on the heated stage (37 °C) of an inverted confocal laser microscope (model LSM510 META, Carl Zeiss, Jena, Germany). The excitation was 515 nm and the emissions were 645 nm and 592 nm. The fluorescence ratio (F645/F592) was calculated. The calibration was performed using the cells perfused with the calibration solutions to obtain the calibration line. The pH_i of ciliary cell was calculated from the calibration line. The calibration solution contained 110 mM KCl, 25 mM $KHCO_3$, 11 mM glucose, 1 mM $MgCl_2$, 1 mM $CaCl_2$, 10 mM HEPES, and 10 μM nigericin and was aerated with 95% O_2 and 5% CO_2. The pH of calibration solution was adjusted to 6.8, 7.2, 7.4, 7.6, or 7.8 by adding 1 M CsOH at 37 °C [12, 15, 16, 35].

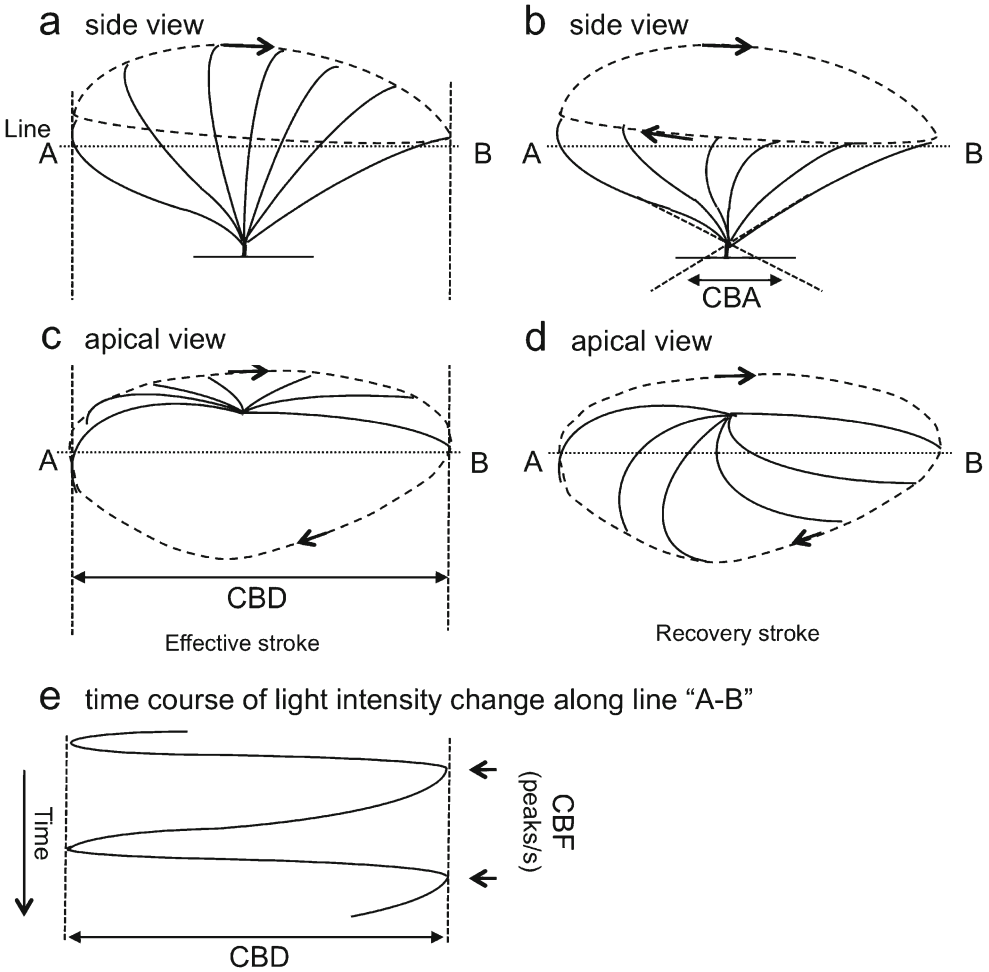

Fig. 1 Beating cycle of airway cilium seen from the side and the top. **a**, **b** Side view of the **a** effective stroke and **b** recovery stroke. The cilium of the left side shows the start of effective stroke and that of the right side shows the end of effective stroke. The angle between the start and the end of effective stroke was measured as CBA (**b**). **c**, **d** Apical view of the **a** effective stroke and **b** recovery stroke. **e** The time course of light intensity change along the line "A–B" (**a–d**). To assess the amplitude of ciliary beating, especially in the apical view, we measured the distance between the start and the end of effective stroke in the image showing the light intensity change along the line "A–B", as ciliary beat distance (CBD). The CBD is an index of the amplitude of ciliary beating. The number of peaks for 1 s shows CBF

Statistical analysis

Statistical significance was assessed by the analysis of variance (ANOVA) or Student's *t* test, as appropriate. Differences were considered significant at $p < 0.05$.

Results

The cells were first perfused with the CO_2/HCO_3^--containing control solution for 5 min and then, with the CO_2/HCO_3^--free control solution. The previous study demonstrated that the HCO_3^--containing Cl^--free NO_3^- solution activates Na^+–HCO_3^- cotransport (NBC) leading to increase CBD and CBF by elevating pH_i in airway ciliary cells [15]. On the other hand, under the CO_2/HCO_3^--free condition, NBC and AE (Cl^-/HCO_3^- exchange) do not function, because of no HCO_3^-. Therefore, in this study, all the experiments were carried out under the CO_2/HCO_3^--free condition.

Effects of Cl^--free solution on CBD, CBA, CBF, and $[Ca^{2+}]_i$

Figure 2a shows the video images of a cHNEC in primary culture, and the beating cilia were observed from the apical side in the CO_2/HCO_3^--free control solution. Panels a1 and a2 show the end and the start of an effective stroke, respectively. Figure 2c shows the time course of changes in light intensity along a line "A–B" on a beating cilium (Fig. 2a); the distance from "line S" to "line E" shows CBD ("←→" in Fig. 2c). In this case, the value of CBD was 70 pixels. Figure 2b shows the video images of the same cHNEC 15 min after switch to the Cl^--free NO_3^- solution, keeping CO_2/HCO_3^--free condition. Panels b1 and b2 show the end and the start of an effective

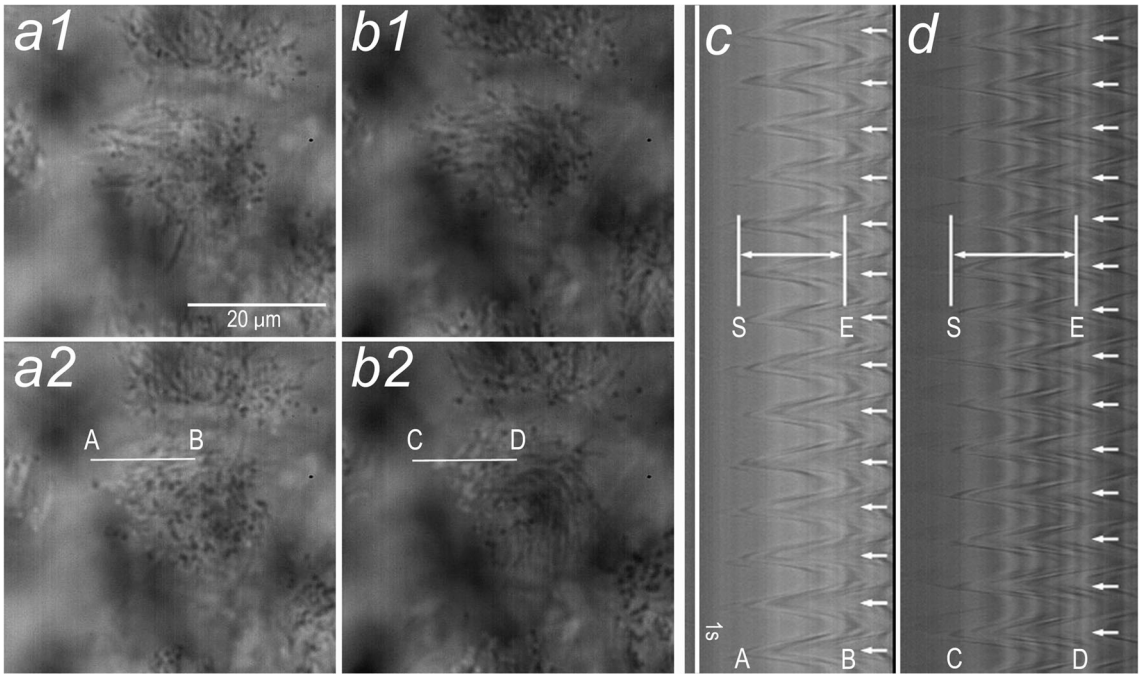

Fig. 2 Video images of ciliated human nasal epithelial cells (cHNECs) (apical view). The cHNECs were set in the perfusion chamber mounted on an inverted microscope equipped with a high-speed camera. Cells were observed using an objective lens (×60). **a**, **b** The cHNECs were perfused with the CO_2/HCO_3^--free control solution for 10 min (**a**) and then, with the Cl^--free NO_3^- solution for further 15 min (**b**). Panels show the start (**a1**, **b1**) and the end (**a2**, **b2**) of effective stroke in a ciliary beating cycle, respectively. When we set a line on the beating cilium on the video images (white lines "A–B" and "C–D" in panels **a2** and **b2**, respectively), the analysis program reported the changes in light intensity along these lines (**c**, **d**). **c** Changes in the light intensity along the line "A–B" (**a2**) in an unstimulated cHNEC. The reported image shows CBF and CBD. Two white lines (**c**) show both the start ("S") and end ("E") of the effective stroke. We measured the distance (pixels) between two lines (←→) as CBD. The arrows (←) show the CBF. **d** Changes in the light intensity along the line "C–D" in the cHNEC perfused with the Cl^--free NO_3^- solution for 15 min. The reported image clearly shows that the Cl^--free NO_3^- solution increased CBD, but not CBF. The arrows (←) show the CBF

stroke, respectively. Figure 2d shows the time course of changes in the light intensity along a line "C–D" on the same cilium (Fig. 2b). The value of CBD ("←→" in Fig. 2d) was 103 pixels. The reported images (Fig. 2c, d) also show CBF. The number of peaks marked by white arrows shows CBF. In this case, CBF in the control solution was 14 Hz (Fig. 2c) and was also 14 Hz in the Cl^--free NO_3^- solution (Fig. 2d). Thus, application of the Cl^--free NO_3^- solution increased CBD, but not CBF, in cHNECs.

We also measured CBA using a side view of cHNECs just before (Fig. 3a) and 15 min after application of the Cl^--free NO_3^- solution (Fig. 3b). The white lines indicate the start (Fig. 3a1) and the end positions of an effective stroke (Fig. 3a2) in a ciliary beating cycle. The white line in Fig. 3a1 was superimposed on Fig. 3a2, and the angle between two lines shows CBA [20]. Similarly, Fig. 3b1, b2 show the CBA in the cHNEC 15 min after application of the Cl^--free NO_3^- solution, demonstrating that the Cl^--free NO_3^- solution increases CBA.

Application of the Cl^--free NO_3^- solution decreases $[Cl^-]_i$ in airway ciliary cells [13–16]. We monitored changes in $[Cl^-]_i$ of cHNECs using MQAE fluorescence intensity. Figure 3c, d show MQAE-fluorescence images of cHNEC just before and 15 min after application of the Cl^--free NO_3^- solution. Application of the Cl^--free NO_3^- solution increased the intensity of MQAE fluorescence, indicating that the Cl^--free NO_3^- solution decreased $[Cl^-]_i$ in cHNECs as expected. Thus, a decrease in $[Cl^-]_i$ correlates with CBD or CBA, but not CBF, in cHNECs.

Effects of an $[Cl^-]_i$ decrease on CBD and CBF

Figure 4a, which is a typical case, shows changes in CBD and CBF induced by application of the Cl^--free NO_3^- solution in cHNECs. The values of CBD and CBF in the CO_2/HCO_3^--containing control solution were 68–74 pixels and 9 Hz, respectively. Switch to the CO_2/HCO_3^--free control solution increased CBD to 78–80 pixels and decreased CBF only slightly, and the value of CBF 5 min after the switch was 8.5 Hz. Then, switch to the Cl^--free NO_3^-solution immediately increased CBD, but did not change CBF. The values of CBD and CBF 15 min after the switch were 100 pixels and 8.5 Hz, respectively. Changes in the CBD ratio and CBF ratio (CBD and CBF normalized to the control values) are shown in Fig. 4b. Switch to the CO_2/HCO_3^--free control solution

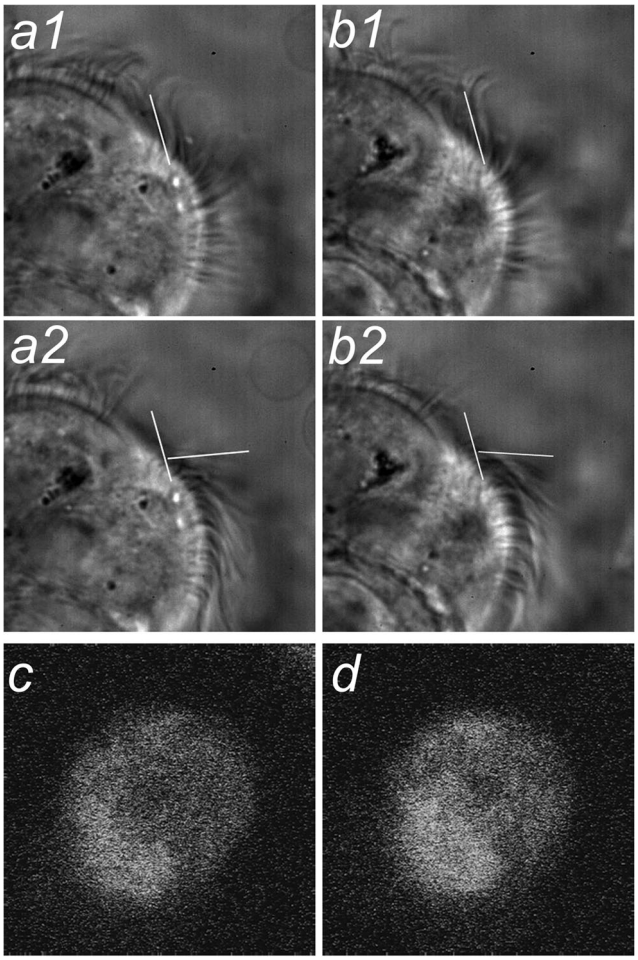

Fig. 3 Video images of cHNECs (side view) and MQAE fluorescence image. **a** Video images of cHNECs during perfusion with the CO_2/HCO_3^--free solution. White lines (**a1** and **a2**) indicate the start and end of an effective stroke in the ciliary beating cycle, respectively. The white line (**a1**) is superimposed (**a2**). The angle between two lines shows the CBA. **b** Video images of cHNECs 15 min after the application of the Cl^--free NO_3^- solution. White lines (**b1** and **b2**) show the start and end of an effective stroke in the ciliary beating cycle. The white line (**b1**) is also superimposed (**b2**). The angle between two lines shows the CBA. The application of the Cl^--free NO_3^- solution increased CBA. **c** The MQAE fluorescence image of a cHNEC during control perfusion in the CO_2/HCO_3^--free solution. **d** The MQAE fluorescence image of a cHNEC 15 min after the application of the Cl^--free NO_3^- solution. The Cl^--free NO_3^- solution potentiated the intensity of MQAE fluorescence, indicating a decrease in $[Cl^-]_i$

increased CBD slightly but not CBF. The values of CBD and CBF ratios 5 min after the switch were 1.07 ± 0.03 (n = 10) and 0.97 ± 0.02 (n = 12), respectively (Fig. 4b). Then, switch to the Cl^--free NO_3^- solution immediately increased CBD ratio, but not CBF ratio. The values of CBD ratio and CBF ratio 6 min after the switch were 1.45 ± 0.03 (n = 10) and 0.97 ± 0.04 (n = 12), respectively (Fig. 4b). Changes in $[Cl^-]_i$ were monitored by the MQAE fluorescence ratio (F_0/F) (Fig. 4c). Switch from the CO_2/HCO_3^--containing control solution to the CO_2/HCO_3^--free control solution decreased F_0/F, and the value of F_0/F 10 min after switch was 0.92 ± 0.01 (n = 9). Then, switch to the Cl^--free NO_3^- solution further decreased F_0/F. The value of F_0/F 10 min after the second switch was 0.77 ± 0.01 (n = 9).

We also measured CBA using the side view of cilia (Fig. 4d). Switch from the CO_2/HCO_3^--containing control solution to the CO_2/HCO_3^--free control solution induced a small increase in CBA, the value of CBA ratio 5 min after the switch was 1.09 ± 0.01 (n = 3) without any increase in CBF (CBF 5 min after the switch = 1.02 ± 0.05, n = 3). Then, switch to the Cl^--free NO_3^- solution increased CBA without any CBF increase, and the value of CBA ratio and CBF ratio 5 min after the switch were 1.37 ± 0.02 (n = 3) and 0.99 ± 0.03 (n = 3). Thus, application of the Cl^--free NO_3^- solution increased CBA similarly to CBD in the cHNEC cell sheet, indicating that CBD is an index of ciliary beating amplitude.

The effects of extracellular Cl^- concentration ($[Cl^-]_o$) on CBD and CBF were examined. Figure 5 shows changes in CBD and CBF of cHNECs, upon changing $[Cl^-]_o$ from 154 mM to 100 mM, 50 mM, and 0 mM by substituting NO_3^- for Cl^-. Decreasing $[Cl^-]_o$, CBD increased, but CBF did not (Fig. 5a). The values of CBD ratio (n = 5) were 1.07 ± 0.01 at 154 mM $[Cl^-]_o$, 1.18 ± 0.01 at 100 mM $[Cl^-]_o$, 1.23 ± 0.01 at 50 mM $[Cl^-]_o$, and 1.36 ± 0.01 at 0 mM $[Cl^-]_o$. Figure 5b shows changes in the MQAE fluorescence ratio (F_0/F) at various $[Cl^-]_o$s. Switch to the CO_2/HCO_3^--free control solution alone decreased F_0/F (Fig. 5b). The CO_2/HCO_3^--free solution appears to decrease NaCl entry via inhibition of NBC and AE, leading to an $[Cl^-]_i$ decrease [15]. The MQAE fluorescence ratio (F_0/F) 5 min after the switch (n = 5) was 1.07 ± 0.01. Then, further reduction of $[Cl^-]_o$ decreased F_0/F. The values of F_0/F were 1.18 ± 0.01 at 100 mM $[Cl^-]_o$, 1.23 ± 0.01 at 50 mM $[Cl^-]_o$, and 1.36 ± 0.01 at 0 mM $[Cl^-]_o$. Decreasing $[Cl^-]_o$, the value of F_0/F decreased.

To decrease $[Cl^-]_i$, we used an inhibitor of $Na^+/K^+/2Cl^-$ cotransport (20 μM bumetanide). In the CO_2/HCO_3^--free solution, the values of CBD ratio and CBF ratio just before addition of bumetanide were 1.08 ± 0.01 (n = 5) and 1.00 ± 0.02 (n = 5), respectively. Addition of bumetanide (20 μM) increased CBD, but not CBF, similar to the Cl^--free NO_3^- solution (Fig. 6a). The values of CBD ratio and CBF ratio 5 min after addition of bumetanide were 1.33 ± 0.03 (n = 5) and 0.97 ± 0.03 (n = 5). Changes in $[Cl^-]_i$ induced by bumetanide were monitored by the MQAE fluorescence ratio (F_0/F) (Fig. 6b). Switch to the CO_2/HCO_3^--free solution decreased F_0/F, and the value of F_0/F just before addition of bumetanide was 0.96 ± 0.03 (n = 4). Then, addition of bumetanide decreased F_0/F. The value of F_0/F 5 min after bumetanide addition was 0.85 ± 0.02 (n = 4). Thus, addition of bumetanide also increased CBD and decreased F_0/F, although the extents of CBD increase and F_0/F decrease induced by bumetanide were 70% of those induced by application of the Cl^--free NO_3^- solution. This suggests that Cl^- entered cHNECs via

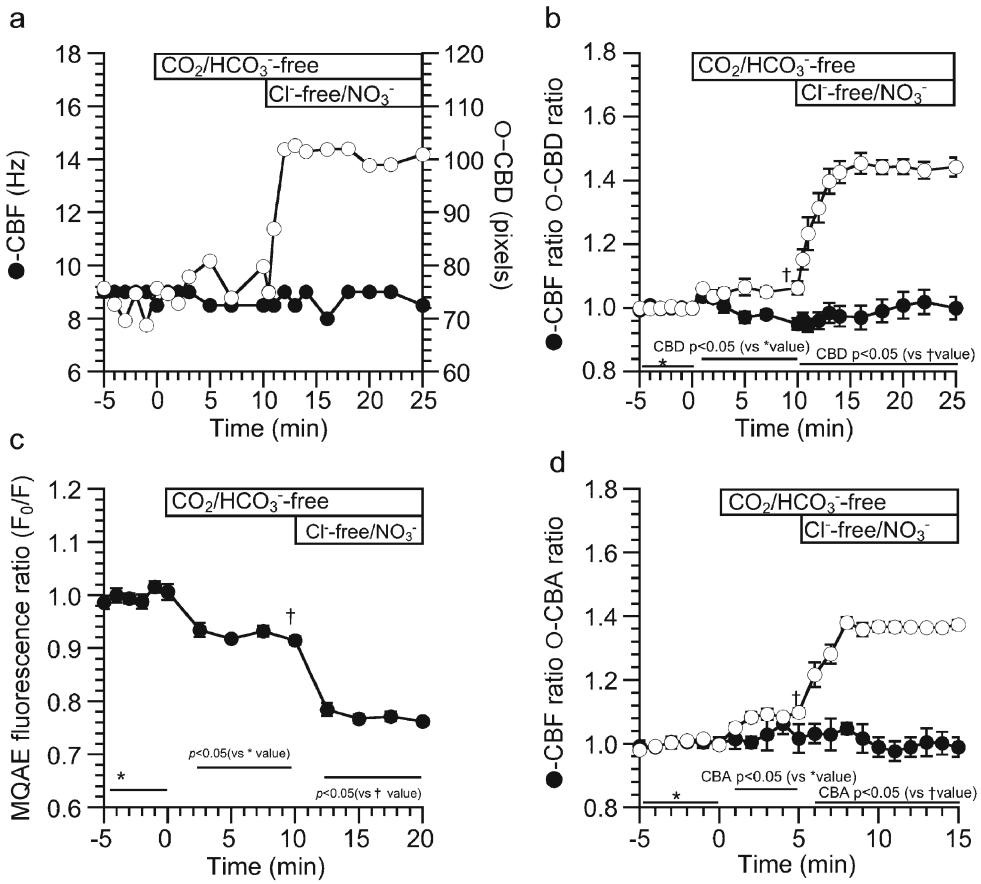

Fig. 4 The effects of Cl^--free NO_3^- solution on CBF and CBD in cHNECs. **a** A typical case. The CBD and CBF in the CO_2/HCO_3^--containing control solution were 68–74 pixels and 9 Hz, respectively. The switch to the CO_2/HCO_3^--free control solution increased CBD by 5–8 pixels and decreased CBF by 0.5 Hz. The second switch to a Cl^--free NO_3^- solution immediately increased CBD, which reached a plateau within 2 min, but did not change CBF. The values of CBD and CBF 15 min after the second switch were 100 pixels and 8.5 Hz. **b** Changes in the CBD ratio and the CBF ratio (normalized CBD and CBF). Switch to the CO_2/HCO_3^--free control solution induced a small increase in CBD and a slight decrease in CBF. The values of CBD ratio and CBF ratio 5 min after the switch were 1.07 ± 0.03 (n = 10) and 0.97 ± 0.02 (n = 12), respectively. Then, switch to the Cl^--free NO_3^- solution immediately increased CBD but not CBF. The values of CBD ratio and the CBF ratio 6 min after the switch were 1.45 ± 0.03 (n = 10) and 0.97 ± 0.04 (n = 12), respectively. **c** Changes in MQAE fluorescence ratio (F_0/F). Switch to the CO_2/HCO_3^--free control solution decreased F_0/F (the value of F_0/F 10 min after the switch was 0.92 ± 0.01, n = 9). Then, switch to the NO_3 solution further decreased F_0/F. The value of F_0/F 10 min after the second switch was 0.76 ± 0.01 (n = 9). **d** Changes in CBA ratio and CBF ratio (normalized CBA and CBF) induced by the Cl^--free NO_3^- solution in cHNECs. Switch to the CO_2/HCO_3^--free control solution induced a small increase in CBA, and then, switch to the Cl^--free NO_3^- solution further increased CBA but not CBF

the $Na^+/K^+/2Cl^-$ cotransport under the CO_2/HCO_3^--free condition.

Previous studies suggested that a decrease in $[Cl^-]_i$ increased CBF in airway ciliary cells of rat [30]. Moreover, in the previous studies, an activation of Cl^- secretion, which decreases $[Cl^-]_i$, increased CBF [3, 15, 16]. Thus, results of the previous studies appear to be inconsistent with that of the present experiments. However, our recent study revealed that a $[Cl^-]_i$ decrease increases CBF at 25 °C [16]. The previous studies were carried out at room temperature or under not well-controlled temperature conditions. We examined the effects of Cl^--free NO_3^- solution on CBD and CBF of cHNECs under the CO_2/HCO_3^--free condition at 25 °C. Application of the Cl^--free NO_3^- solution increased both CBD and CBF under the CO_2/HCO_3^--free condition at 25 °C (Fig. 6c). The values of CBD and CBF ratios just before application of the Cl^--free NO_3^- solution were 1.06 ± 0.01 (n = 5) and 1.01 ± 0.01 (n = 5), and those 5 min after the application were 1.30 ± 0.02 (n = 5) and 1.14 ± 0.02 (n = 5). Thus, the effects of a low $[Cl^-]_i$ on CBF depend on the temperature in cHNECs,

Effects of NPPB on CBD and CBF

To increase $[Cl^-]_i$, cHNECs were treated with NPPB (20 μM, a Cl^- channels blocker). NPPB inhibits the Cl^- release from cells to increase $[Cl^-]_i$ [13–16]. The switch to the CO_2/HCO_3^--free control solution immediately increased CBD (CBD ratio 10 min after the switch = 1.10 ± 0.03, n = 6), but

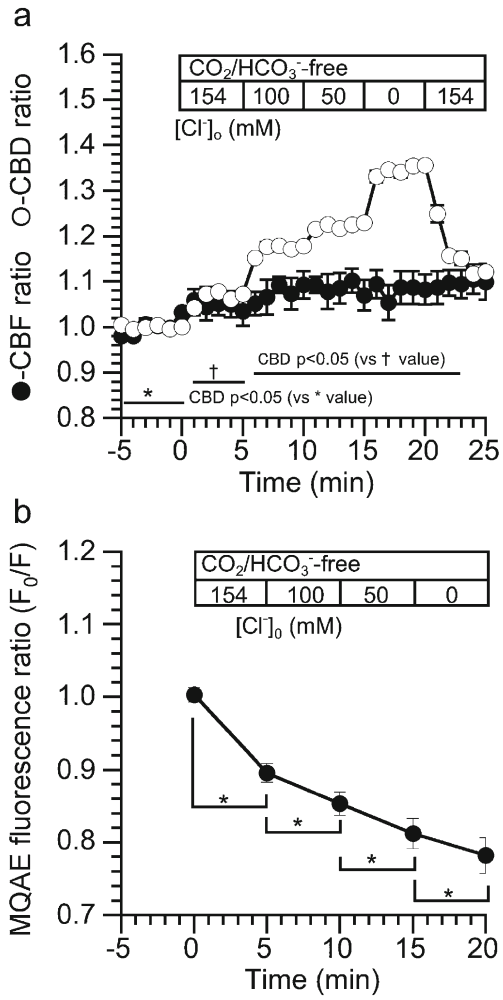

Fig. 5 Effects of various extracellular Cl^- concentrations ($[Cl^-]_o$s) on CBD and CBF in cHNECs. The cHNECs were first perfused with the CO_2/HCO_3^--containing control solution for 5 min and then with the CO_2/HCO_3^--free control solution. Experiments were carried out under the CO_2/HCO_3^--free condition. **a** Changes in CBD and CBF at various $[Cl^-]_o$s (154 mM, 100 mM, 50 mM, and 0 mM). Decrements of $[Cl^-]_o$, increased CBD, but not CBF. **b** MQAE fluorescence ratio (F_0/F) changed by various $[Cl^-]_o$s. The experimental protocol was the same (**a**). Switch to the CO_2/HCO_3^--free control solution decreased F_0/F. As decrement of $[Cl^-]_o$, MQAE fluorescence ratio (F_0/F) decreased

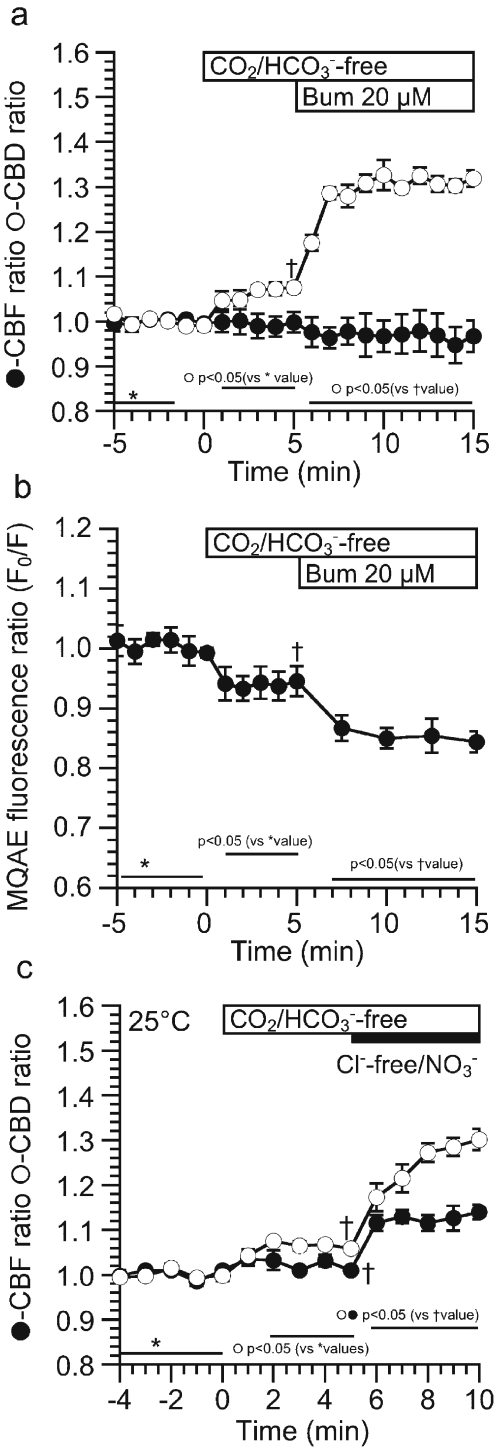

Fig. 6 Changes in CBD, CBF, and MQAE fluorescence ratio (F_0/F) induced by bumetanide. **a** Changes in CBD and CBF. Switch to the CO_2/HCO_3^--free solution increased CBD, but not CBF. Addition of bumetanide (20 μM) increased CBD but not CBF. **b** Changes in F_0/F (MQAE fluorescence ratio). Switch to the CO_2/HCO_3^--free solution decreased F_0/F. Addition of bumetanide (20 μM) decreased F_0/F. **c** Changes in CBD and CBF induced by the Cl^--free NO_3^- solution at 25 °C. Switch to the CO_2/HCO_3^--free solution increased CBD, but not CBF. Application of the Cl^--free NO_3^- solution increased both CBD and CBF at 25 °C

not CBF (CBF ratio 10 min after the switch = 0.97 ± 0.01, n = 6, not significant) (Fig. 7a). Then, addition of NPPB immediately decreased CBD and gradually CBF. The values of CBD ratio and CBF ratio 15 min after NPPB addition were 0.73 ± 0.02 (n = 6) and 0.81 ± 0.02 (n = 6) (Fig. 7a). Changes in $[Cl^-]_i$ were monitored by the MQAE fluorescence ratio (F_0/F) (Fig. 7b). Switch to the CO_2/HCO_3^--free solution decreased F_0/F and the value of F_0/F just before addition of NPPB was 0.93 ± 0.02 (n = 7). Addition of NPPB increased F_0/F and the value of F_0/F 5 min after the addition was 1.18 ± 0.03 (n = 7). Thus, an increase in $[Cl^-]_i$ correlates with decreases in both CBD and CBF in cHNECs.

The effects of a CFTR inhibitor, CFTR(inh)-172 (1 μM), on CBF, CBD, and $[Cl^-]_i$ were examined. Under the CO_2/HCO_3^--free condition, the addition of CFTR(inh)-172 (1 μM) decreased CBD and CBF (Fig. 7c). The values of CBD ratio and CBF ratio before the addition of CFTR(inh)-172 were 1.00 ± 0.01 ($n = 7$) and 0.99 ± 0.00 ($n = 5$) and those 5 min after the addition were 0.80 ± 0.03 ($n = 7$) and 0.88 ± 0.01 ($n = 5$), respectively. Changes in $[Cl^-]_i$ were monitored using MQAE fluorescence (Fig. 7d). Under the CO_2/HCO_3^--free solution, the addition of CFTR(inh)-172 increased F_0/F, similarly NPPB. The value of F_0/F just before the addition was 0.96 ± 0.02 ($n = 7$), and that 10 min after the addition was 1.12 ± 0.03 ($n = 7$).

Effects of CO_2/HCO_3^--free solution on CBD, CBF, and pH_i

Previous studies exhibited that switch to the CO_2/HCO_3^--free control solution increases pH_i in lung and airway epithelial cells [32, 35]. Moreover, an elevation of pH_i increases CBA and CBF in airway ciliary cells [15, 32]. However, in cHNECs, switch to the CO_2/HCO_3^--free control solution induced a small CBD increase and a small transient CBF increase (Fig. 8a). The value of CBD ratio 5 min after the switch was 1.09 ± 0.01 ($n = 32$), and the value of CBF ratio 1 min after the switch was 1.02 ± 0.01 ($n = 63$), and those 5 min and 10 min after the switch were 1.01 ± 0.01 ($n = 63$) and 0.99 ± 0.01 ($n = 32$). The extents of CBD and CBF increase evoked

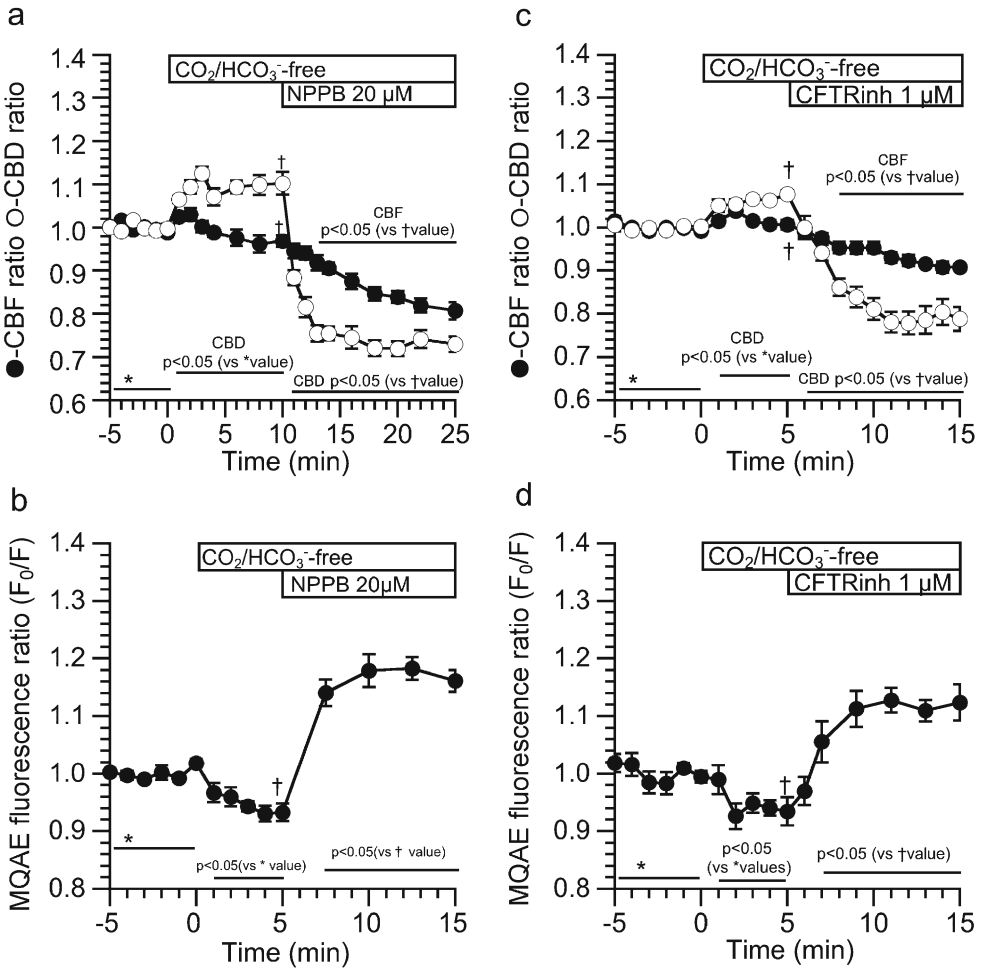

Fig. 7 Effects of NPPB on CBD, CBF, and MQAE fluorescence ratio (F_0/F) in cHNECs. The cHNECs were first perfused with CO_2/HCO_3^--containing control solution and then with CO_2/HCO_3^--free control solution. **a** Changes in CBD ratio and CBF ratio induced by 20 μM NPPB in cHNECs. The addition of 20 μM NPPB evoked an immediately decrease followed by a gradual decrease in CBD. **b** Changes in MQAE fluorescence ratio (F_0/F) induced by NPPB. The switch to the CO_2/HCO_3^--free control solution decreased F_0/F. Then, the addition of 20 μM NPPB increased the F_0/F, which reached a plateau within 5 min. **c** Effects of a CFTR inhibitor, CFTR(inh)-172 (1 μM), on CBF and CBD. Under the CO_2/HCO_3^--free condition, the addition of CFTR(inh)-172 (1 μM) decreased CBD and CBF. The values of CBD ratio and CBF ratio before the addition of CFTR(inh)-172 were 1.00 ± 0.01 ($n = 7$) and 0.99 ± 0.00 ($n = 5$) and those 5 min after the addition were 0.80 ± 0.03 ($n = 7$) and 0.88 ± 0.01 ($n = 5$), respectively. **d** Changes in $[Cl^-]_i$. Under the CO_2/HCO_3^--free solution, the addition of CFTR(inh)-172 increased F_0/F. The value of F_0/F just before the addition was 0.96 ± 0.02 ($n = 7$) and that 10 min after the addition was 1.12 ± 0.03 ($n = 7$)

by application of the CO_2/HCO_3^--free control solution was much less in cHNECs than in human tracheobronchial ciliary cells and mouse airway ciliary cells [32, 35]. Changes in pH_i were measured in cHNECs upon switching to the CO_2/HCO_3^--free control solution (Fig. 8b). In the CO_2/HCO_3^--containing control solution, the pH_i of cHNECs was 7.46–7.47. Switch to the CO_2/HCO_3^--free control solution transiently increased pH_i. The values of pH_i 2 min and 10 min after the switch were 7.57 ± 0.05 and 7.43 ± 0.07 ($n = 6$), respectively. However, the extent of transient pH_i increase ($\Delta pH_i = 0.09$) was much less in cHNECs than in human tracheobronchial ciliary cells ($\Delta pH_i = 0.51$) [32].

To examine the small elevation of pH_i by application of the CO_2/HCO_3^--free control solution, we used an inhibitor of carbonic anhydrase (CA), acetazolamide (100 μM, A-amide) to inhibit H^+ production from CO_2. Addition of A-amide did not change CBD and CBF in the presence of CO_2/HCO_3^-. Then, switch to the CO_2/HCO_3^--free solution also did not change CBD and CBF. Further application of the Cl^--free NO_3^- solution, keeping the CO_2/HCO_3^--free condition, increased CBD, but not CBF (Fig. 8c). Thus, A-amide did not inhibit CBD increase induced by Cl^--free NO_3^- solution, although it inhibited CBD increase induced by the CO_2/HCO_3^- solution. Changes in pH_i were measured in the presence of A-amide. Addition of A-amide did not change pH_i in the CO_2/HCO_3^--containing control solution, and then, switch to the CO_2/HCO_3^--free solution also did not change pH_i. Further application of the Cl^--free NO_3^- solution, keeping the CO_2/HCO_3^--free condition, slightly decreased pH_i (Fig. 8d). This observation suggests that H^+ excretion via transporters, such

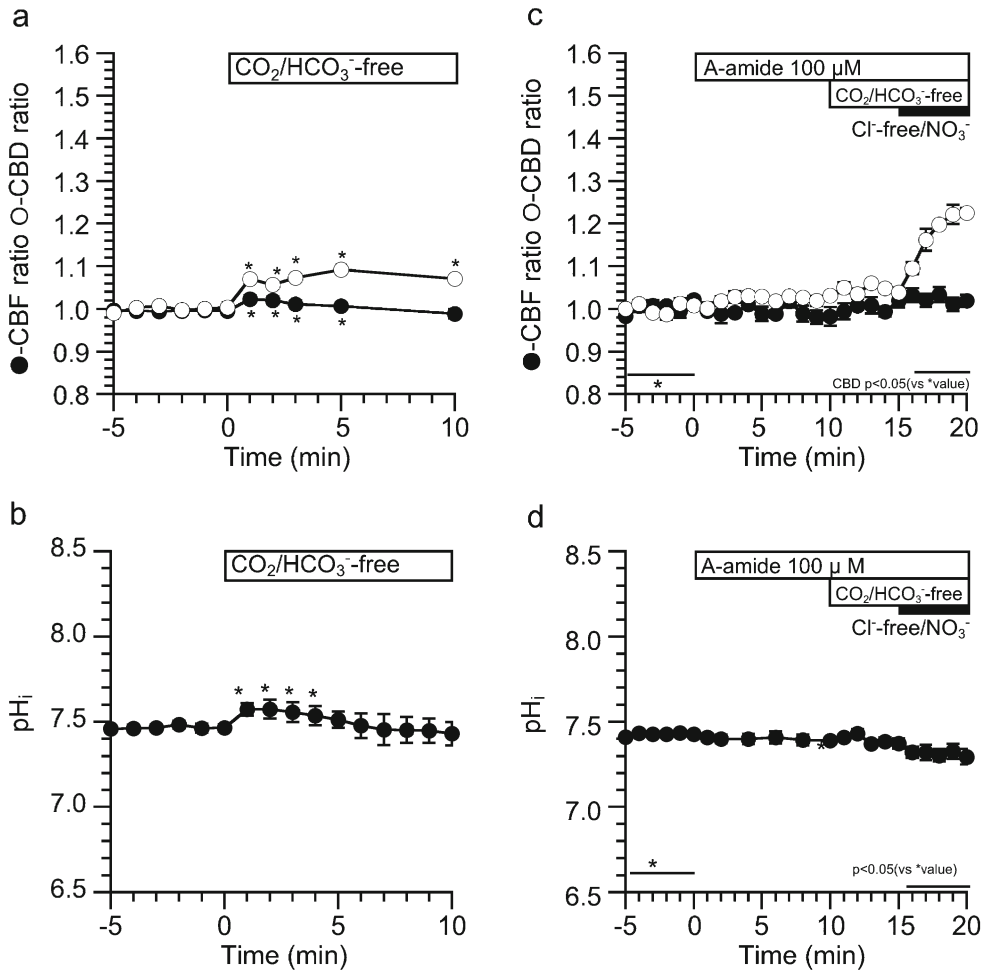

Fig. 8 Effects of acetazolamide (a carbonic anhydrase inhibitor) on changes in CBD, CBF, and pH_i induced by the CO_2/HCO_3^--free control solution. **a** Changes in CBD and CBF induced by the CO_2/HCO_3^--free solution. Switch to the CO_2/HCO_3^--free control solution induced a sustained increase in CBD and a small transient increase in CBF. **b** Changes in pH_i. In the CO_2/HCO_3^--containing control solution, pH_i of cHNECs was 7.46–7.47. Switch to the CO_2/HCO_3^--free control solution transiently increased pH_i, and pH_i returned to the control level within 5 min. The transient peak value of pH_i was 7.57 ± 0.05 ($n = 6$) and pH_i 10 min after the switch was 7.43 ± 0.07 ($n = 6$). **c** Changes in CBD and CBF induced by the CO_2/HCO_3^--free solution in the presence of acetazolamide (100 μM). In the presence of acetazolamide, switch to the CO_2/HCO_3^--free control solution did not induce any change in CBD and CBF. However, further switch to the Cl^--free NO_3^- solution increased CBD. **d** Changes in pH_i induced by the CO_2/HCO_3^--free solution in the presence of acetazolamide (100 μM). Acetazolamide abolished the pH_i changes induced by the CO_2/HCO_3^--free solution

as Na^+/H^+ exchange, is negligibly small in cHNECs under this experimental condition.

To examine the effects of pH_i elevation on CBD and CBF in cHNECs, the NH_4^+ pulse (addition of 25 mM NH_4Cl) was applied under the CO_2/HCO_3^--free condition (Fig. 9) [32, 35]. Switch to the CO_2/HCO_3^--free solution induced a small CBD increase and a slight and transient CBF increase. The values of CBD 5 min after switch to the CO_2/HCO_3^--free solution were 1.07 ± 0.01 ($n = 5$) and those of CBF 1 min and 5 min after switch to the CO_2/HCO_3^--free solution were 1.03 ± 0.02 and 0.97 ± 0.02 ($n = 6$). Then, application of the NH_4^+ pulse induced a rapid increase followed a small gradual decrease in CBD and CBF (Fig. 9a). The values of CBD 1 min and 5 min after application of the NH_4^+ pulse were 1.26 ± 0.04 and 1.21 ± 0.03 ($n = 5$) and those of CBF 2 min and 5 min after application of the NH_4^+ pulse were 1.08 ± 0.03 and 1.11 ± 0.03 ($n = 6$). Changes in pH_i were measured upon applying the NH_4^+ pulse. Switch to the CO_2/HCO_3^- solution induced a small transient pH_i increase. The values of pH_i 2 min and 5 min after the switch were 7.70 ± 0.04 and 7.53 ± 0.03 (n-8). Further application of the NH_4^+ pulse induced a transient pH_i increase, an immediate increase followed by a large rapid decrease. The values of pH_i 1 min and 5 min after application of the NH_4^+ pulse were 8.04 ± 0.03 and 7.62 ± 0.05 (n-8).

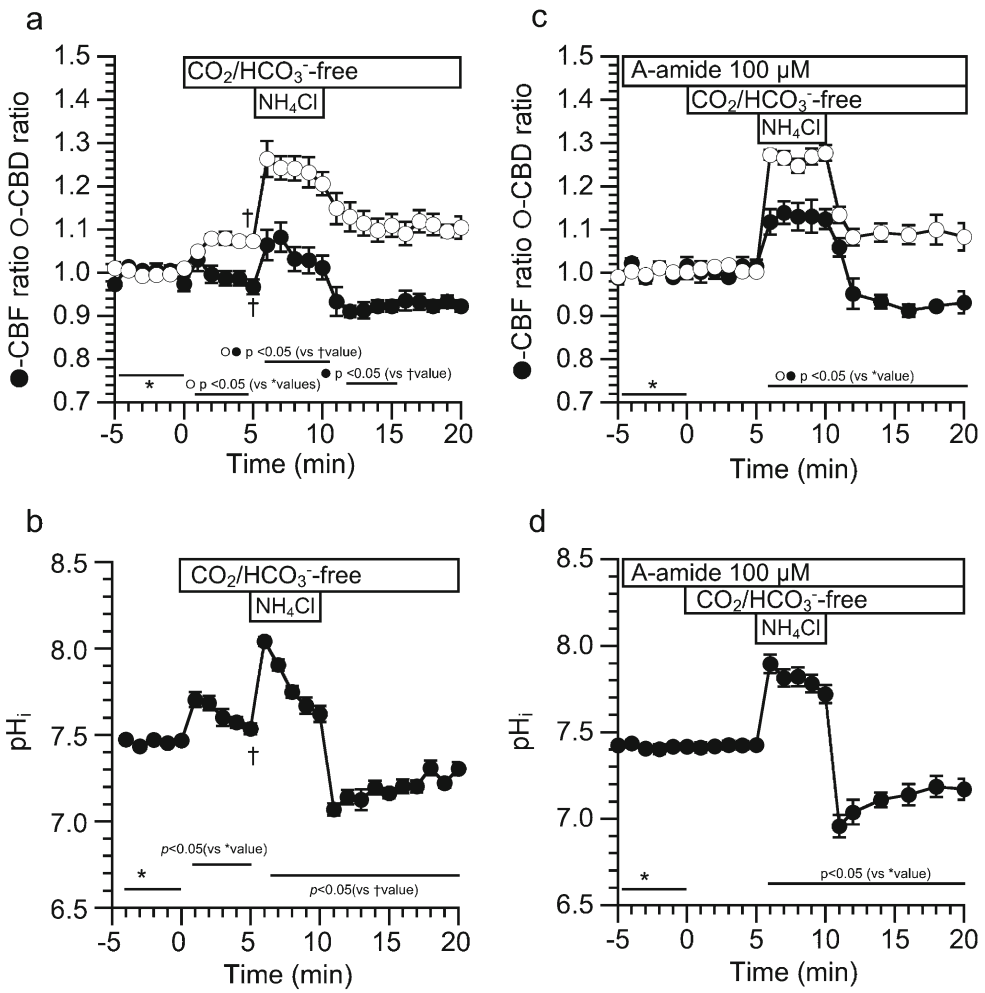

Fig. 9 Effects of acetazolamide (a carbonic anhydrase inhibitor) on changes in CBD, CBF, and pH_i induced by the NH_4^+ pulse. **a** Changes in CBD and CBF induced by the NH_4^+ pulse. Switch to the CO_2/HCO_3^--free control solution induced a sustained increase in CBD and a small transient increase in CBF. Application of the NH_4^+ pulse immediately increased and then slightly decreased CBD (not significant), and it also increased CBF and then gradually decreased (not significant). Removal of the NH_4^+ pulse immediately decreased both CBD and CBF. **b** Changes in pH_i induced by the NH_4^+ pulse. Switch to the CO_2/HCO_3^--free control solution increased a small transient increase in pH_i. Application of the NH_4^+ pulse immediately increased and then rapidly decreased pH_i. Removal of the NH_4^+ pulse immediately decreased and then gradually returned pH_i to the control value. **c** Changes in CBD and CBF induced by the NH_4^+ pulse in the presence of acetazolamide (100 μM). Addition of acetazolamide (100 μM) did not change CBD and CBF, and then, switch to the CO_2/HCO_3^--free control solution also did not change them. Application of the NH_4^+ pulse immediately increased and sustained CBD and CBF. Then, removal of the NH_4^+ pulse decreased CBD and CBF. **d** Changes in pH_i induced by the NH_4^+ pulse in the presence of acetazolamide (100 μM). Addition of acetazolamide did not change pH_i, and then, switch to the CO_2/HCO_3^--free control solution also did not change it. Application of the NH_4^+ pulse immediately increased and then gradually, not rapidly, decreased pH_i. Removal of the NH_4^+ pulse immediately decreased and then gradually returned pH_i to the control value

Removal of the NH_4^+ pulse induced an immediate decrease followed by a gradual recovery in pH_i (Fig. 9b). The values of pH_i 1 min and 5 min after removal of the NH_4^+ pulse were 7.07 ± 0.04 and 7.16 ± 0.03 (n-8).

Experiments were also carried out in the presence of A-amide (100 μM). Addition of A-amide did not change CBD and CBF, and then, switch to the CO_2/HCO_3^--free control solution did not change CBD and CBF. The values of CBD and CBF just before application of the NH_4^+ pulse were 1.00 ± 0.01 ($n = 5$) and 1.01 ± 0.02 (n-5). Application of the NH_4^+ pulse increased and sustained both CBD and CBF (Fig. 9c). The values of CBD and CBF 5 min after the NH_4^+ pulse were 1.28 ± 0.02 ($n = 5$) and 1.12 ± 0.02 (n-5). Removal of the NH_4^+ pulse immediately decreased both CBD and CBF. The values of CBD and CBF 6 min after removal of the NH_4^+ pulse were 1.09 ± 0.02 ($n = 5$) and 0.91 ± 0.01 (n-5). Changes in pH_i were measured in the presence of A-amide (Fig. 9d). Addition of A-amide and further application of the CO_2/HCO_3^--free control solution did not induce any change in pH_i. The value of pH_i just before application of the NH_4^+ pulse was 7.43 ± 0.02 ($n = 7$). Application of the NH_4^+ pulse induced an immediate increase followed by a small gradual decrease in pH_i. The values of pH_i 1 min and 5 min after application of the NH_4^+ pulse were 7.89 ± 0.06 and 7.72 ± 0.05 ($n = 7$). Removal of the NH_4^+ pulse induced an immediate decrease followed by a gradual recovery in pH_i. The values of pH_i 1 min and 6 min after removal of the NH_4^+ pulse were 6.96 ± 0.07 and 7.14 ± 0.06 ($n = 7$). Thus, A-amide inhibited the large rapid decrease following to the immediate increase in pH_i induced by application of the NH_4^+ pulse, suggesting that the large rapid pH_i decrease during application of the NH_4^+ pulse (Fig. 9b) is caused by H^+ production from CO_2 via CA. A large amount of CO_2 appears to be produced in cHNECs, probably via cellular metabolisms, because no CO_2 is supplied from extracellular fluid under the CO_2/HCO_3^--free condition.

Effects of a low $[Cl^-]_i$ on micro-bead movements driven by beating cilia of cHNECs

Previous studies demonstrated that an increase in CBD enhances movements of the micro-bead in cHNECs and lung airway ciliary cells [16, 20]. The distances, that the micro-beads were moved by the surface fluid flow driven by the beating cilia of cHNECs, were measured in the Cl^--containing control solution and in the Cl^--free NO_3^- solution under the CO_2/HCO_3^--free condition (Fig. 10). Switch from the control solution to the Cl^--free NO_3^- solution enhanced the micro-beads movement. The distance of micro-bead moved driven by the beating cilia for 100 ms in the Cl^--containing control solution was 26.0 ± 1.9 μm ($n = 11$) and that in the Cl^--free NO_3^- solution was 36.9 μm ± 3.4 ($n = 10$). Thus, application of the Cl^--free NO_3^- solution, which increases CBD, enhanced the movement of micro-beads in cHNECs.

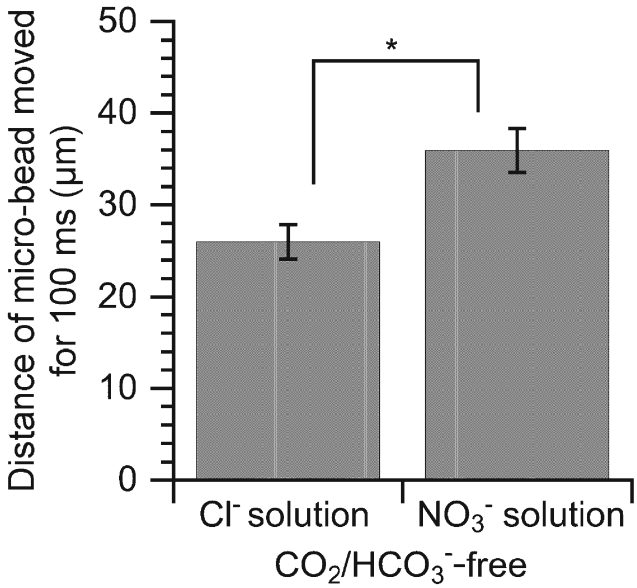

Fig. 10 Enhancement of micro-beads movement driven by ciliary beating of cHNECs induced by the Cl^--free NO_3^- solution. The distances, that the micro-beads were moved by the surface fluid flow driven by the beating cilia of cHNECs, were measured in the control (Cl^--containing) solution and in the Cl^--free NO_3^- solution under the CO_2/HCO_3^--free condition. The distance of micro-bead moved driven by the beating cilia for 100 ms in the Cl^--containing control solution was 26.0 ± 1.9 μm ($n = 11$) and that in the Cl^--free NO_3^- solution was 36.9 μm ± 3.4 ($n = 10$). The Cl^--free NO_3^- solution, which increases CBD in cHNECs, enhanced the movement of micro-beads

Effects of a decrease in $[Cl^-]_i$ on CBF and CBD in cHNECs from chronic sinusitis and from allergic rhinitis

We measured CBF of cHNECs obtained from patients having chronic sinusitis and allergic rhinitis. Experiments were carried out in the CO_2/HCO_3^--containing control solution. The mean CBF in cHNECs from chronic sinusitis was 9.52 ± 0.09 Hz ($n = 364$ cells from 10 patients, Fig. 11a), and that from allergic rhinitis was 9.60 ± 0.08 Hz ($n = 398$ cells from 11 patients, Fig. 11b). There was no significant difference in the basal CBFs of cHNECs obtained from both types of patients. We also examined the effect of the Cl^--free NO_3^- solution on CBF and CBD under the CO_2/HCO_3^--free condition. In cHNECs from patients contracting chronic sinusitis, the switch to the CO_2/HCO_3^--free control solution increased CBD slightly, but not CBF. The CBD ratio and CBF ratio 5 min after the switch were 1.04 ± 0.03 ($n = 8$) and 0.97 ± 0.02 ($n = 5$), respectively. Then, switch to the Cl^--free NO_3^- solution immediately increases CBD, but not CBF. The CBD and CBF ratios 10 min after the switch were 1.43 ± 0.03 ($n = 8$) and 1.04 ± 0.06 ($n = 5$), respectively (Fig. 11c). In cHNECs from patients contracting allergic rhinitis, the switch to the CO_2/HCO_3^--free control solution increased CBD slightly, but not CBF. The CBD and CBF ratios 5 min after the switch were 1.15

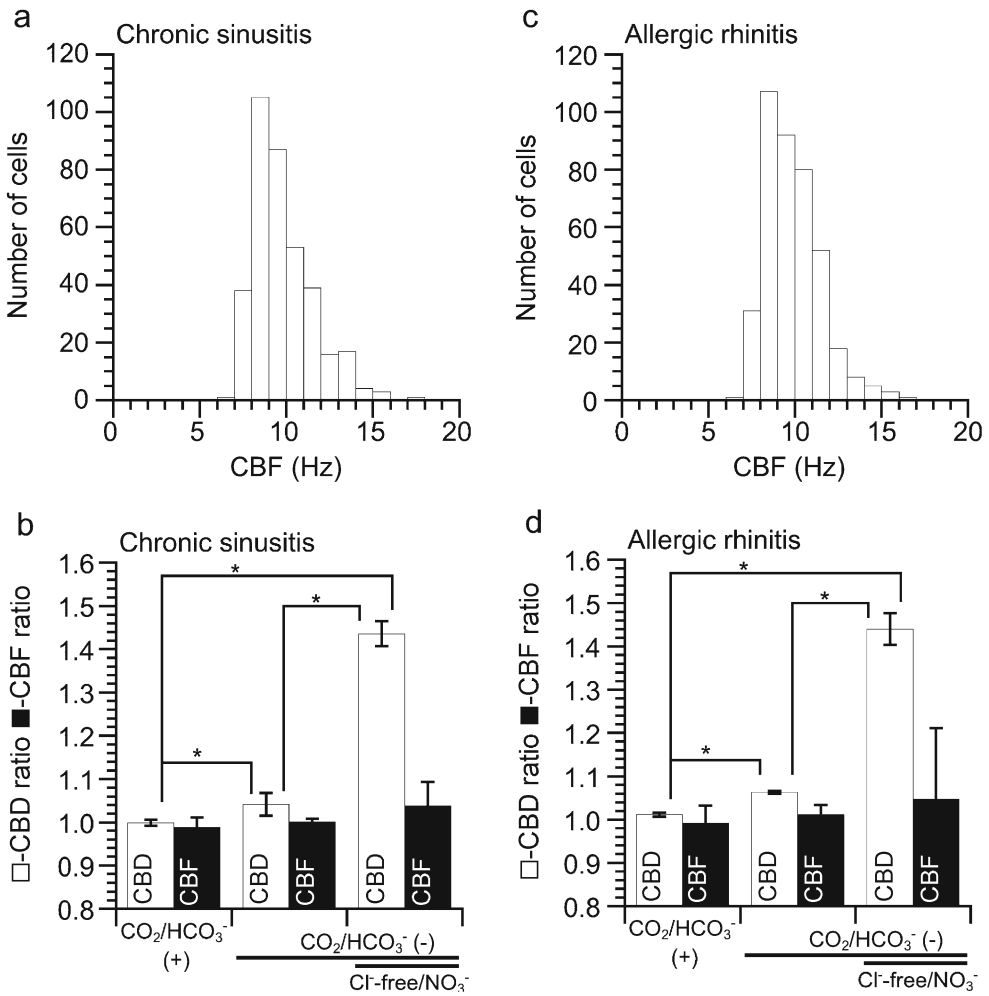

Fig. 11 Distribution of CBF in cHNECs in the CO_2/HCO_3^--containing control solution. The columns refer to the numbers of cells. CBF was measured from cHNECs from the patients requiring surgery. **a** Chronic sinusitis. The mean CBF was 9.52 ± 0.09 Hz (n = 364 cells from 10 patients). **b** Allergic rhinitis. The mean CBF was 9.60 ± 0.08 Hz (n = 398 cells from 11 patients). **c** Changes in the CBD ratio and the CBF ratio in cHNECs from chronic sinusitis patients. The switch to the CO_2/HCO_3^--free control solution induced a small increase in CBD but not CBF. The CBD ratio and CBF ratio 5 min after the switch were 1.04 ± 0.03 (n = 8) and 0.97 ± 0.02 (n = 5). The second switch to the Cl^--free NO_3^- solution immediately increase CBD but not CBF. The CBD and the CBF ratios 10 min after the switch were 1.43 ± 0.03 (n = 8) and 1.04 ± 0.06 (n = 5), respectively. **d** Changes in the CBD ratio and the CBF ratio in cHNECs from allergic rhinitis patients. The switch to the CO_2/HCO_3^--free control solution induced a small increase in CBD but not CBF. The CBD and CBF ratios 5 min after the switch were 1.15 ± 0.02 (n = 3) and 0.91 ± 0.12 (n = 3). The second switch to the Cl^--free NO_3^- solution immediately increase CBD but not CBF. The CBD and the CBF ratios 10 min after the switch were 1.44 ± 0.04 (n = 3) and 1.04 ± 0.16 (n = 3), respectively. *Significantly different (p < 0.05). In patients contracting chronic sinusitis or allergic rhinitis, a decrease in $[Cl^-]_i$ enhanced CBD in cHNECs

± 0.02 (n = 3) and 0.91 ± 0.12 (n = 3), respectively. Then, switch to the Cl^--free NO_3^- solution immediately increases CBD, but not CBF. The CBD and CBF ratios 10 min after the switch were 1.44 ± 0.04 (n = 3) and 1.04 ± 0.16 (n = 3), respectively (Fig. 11d). Increases in CBD in response to application of the Cl^--free NO_3^- solution were similar in cHNECs obtained from both types of patients. A decrease in $[Cl^-]_i$ correlates with increases in CBD of cHNECs in patients suffering from chronic sinusitis or allergic rhinitis. We speculate that a decrease in $[Cl^-]_i$ may increase CBD of cHNECs in both types of patients.

Discussion

We developed a new method to measure CBD, as an index of the amplitude of ciliary beating, in cHNECs. A previous study indicated that changes in the light intensity reported by an image analysis program show the amplitude of ciliary beating [15, 16, 39]. The present study clearly showed that CBD is identical to CBA as the parameter for evaluating the amplitude of ciliary beating.

CBF has been measured to assess the activity of ciliary beating. However, little attention has been paid to the amplitude of airway ciliary beating, such as CBA. Our previous

study demonstrated that an increase in CBA alone enhances the micro-beads transport driven by beating cilia in the airway surface [16, 20]. Moreover, the patients with inner dynein arm defects, beating cilia of which show an abnormal waveform but normal CBF, have symptoms of the primary ciliary dyskinesia, such as bronchiectasis, sinusitis, and situs inversus [7]. The spermatozoa from mice or cilia of Tetrahymena lacking inner dynein arms heavy chain 7 gene showed an irregular wave form (a decreased amplitude) and a decreased swim speed [2, 25, 38]. Thus, the amplitude of ciliary beating is a crucial factor controlling the ciliary transport in the airway.

However, the measurement of CBA has some problems. It requires the video-frame images of a beating cycle with high spatial resolution and high time resolution (such as 500 fps) to capture the fine movement of each cilium. This problem has been resolved by the recent development of high-speed camera. However, some researchers are cautious in the CBA measurement, because CBA measurements may be affected by the experimenter bias. However, the new method shown in this study resolves these problems especially the experimenter bias, because the image reported by the image analysis program shows changes in CBD.

A decrease in $[Cl^-]_i$ enhanced only CBD, not CBF, in cHNECs at 37 °C; however, it enhanced both CBD and CBF at 25 °C. Contrary, an increase in $[Cl^-]_i$ decreased both CBD and CBF at 37 °C. The ciliary beating is maintained by molecular motors, dyneins [9]. Beating cilia have two functionally distinct molecular motors, outer dynein arms (ODAs), and inner dynein arms (IDAs); the ODA regulates frequency, CBF, and the IDA regulates wave form including CBD and CBA [4, 5]. The results of this study indicate that a decrease in $[Cl^-]_i$ enhances activities of both IDAs and ODAs, and an increase in $[Cl^-]_i$ inhibits both activities. These observations suggest that intracellular Cl^-s may bind signal molecules controlling ODAs and IDAs to decrease CBF and CBD, and that the Cl^- concentration response curve of CBF may shift high concentrations compared with that of CBD. A recent study revealed that intracellular Cl^- binds to the kinase domain of with-no-lysin kinase (WNKs) regulating renal Na-Cl cotransporter to inhibit its activity [6]. In cilia of cHNECs, WNKs may also play crucial roles for activating ODA or IDA in response to an $[Cl^-]_i$ decrease. Moreover, an in vitro study demonstrated that the range of $[Cl^-]_i$ activating WNK4 is lower than that activating WNK1 or WNK3 [33]. The subtype of WNK-regulating ODA may be different from that regulating IDA. The different subtypes may cause different responses in CBD and CBF upon decreasing $[Cl^-]_i$ in cHNECs.

On the other hand, the modulation of ODAs regulating CBF stimulated by an $[Cl^-]_i$ decrease appears to depend on the temperature. A low temperature, such as 25 °C, may decrease the Cl^- binding affinity of signaling molecules controlling ODAs, such as WNKs [6, 33]. The affinity decreased by a low temperature, such as 25 °C, may increase the activity of ODA, leading to CBF increase.

There are reports showing that a decrease in $[Cl^-]_i$ modulates various cellular functions, such as Na^+-permeable channels [34], Ca^{2+}-regulated exocytosis [31] and airway ciliary beatings [13, 15, 16, 30, 36]. A previous study showed that the microtubules activity in brain cytoplasmic dynein (ATPase activity) is enhanced by a low concentration of KCl, which increases the dynein affinity to the microtubules [29]. Moreover, intracellular Cl^- modulates G proteins [10], and has an inhibitory effect on GTPase activity to stimulate tubulin polymerization [26, 27]. The small G protein Arl13B, which is considered a ciliary marker, localizes to the microtubule doublets of ciliary axoneme [23]. Changes in $[Cl^-]_i$ may affect interactions between tubulin and dynein, leading to change in CBD and CBF [11].

An elevation of pH_i has been shown to increase CBF [13, 15, 16, 32]. A previous study demonstrated that a pH_i elevation induced by the application of CO_2/HCO_3^--free solution ($\Delta pH_i = 0.51$) increased CBF from 5 to 7 Hz in human tracheal ciliary cells. We also observed similar CBF increase in lung airway ciliary cells of mice; application of the CO_2/HCO_3^--free solution ($\Delta pH_i = 0.4$) increased CBF by 35% [15, 32]. The present study demonstrated that pH_i elevation induced by application of the CO_2/HCO_3^--free solution is transient and its extent ($\Delta pH_i = 0.14$) is much less in cHNECs than in the human tracheal ciliary cells. However, a large increase in pH_i induced by the NH_4^+ pulse stimulated a large CBF increase in cHNECs. Thus, upon applying the CO_2/HCO_3^--free solution, the small transient CBF increase is caused by a small elevation of pH_i in cHNECs.

We performed experiments using an inhibitor of carbonic anhydrase (A-amide) to clarify the cause of a small pH_i increase evoked by switch to the CO_2/HCO_3^--free solution in cHNECs. A-amide, alone, did not change pH_i in the CO_2/HCO_3^--containing solution, and it abolished the small change in pH_i induced by switch to the CO_2/HCO_3^--free solution, suggesting that H^+ is produced from CO_2 in cHNECs. Moreover, in the CO_2/HCO_3^--free solution, the NH_4^+ pulse stimulated a large rapid decrease following an immediate increase in pH_i. The large rapid decrease in pH_i was completely inhibited by acetazolamide, indicating that CO_2 is supplied from the intracellular compartment in cHNECs. Because, the experiments were carried out in the absence of CO_2/HCO_3^-. Thus, a large amount of H^+ is produced by CO_2 via metabolisms of cHNECs. Therefore, switch to the CO_2/HCO_3^--free solution evoked a leakage of CO_2 from cHNECs, leading to a decrease in H^+ concentration (a small pH_i increase). A large amount of CO_2 produced via metabolisms plays a crucial role in the maintenance of pH_i in cHNECs, which are exposed to an extremely low CO_2 concentration (0.04%) in the physiological condition.

The cHNECs were obtained from patients suffering from chronic sinusitis and allergic rhinitis. In cHNECs obtained from both types of patients, application of the NO_3^- solution enhances CBD at 37 °C. These results suggest that a decrease in $[Cl^-]_i$ enhances CBD to increase the rate of mucociliary clearance in nasal epithelia of both types of patients. Therefore, substances to decrease $[Cl^-]_i$ may be an effective therapeutic tool for improving or preventing nasal symptoms of both types of patients. Drugs stimulating airway Cl^- secretion, such as β_2-agonists [30, 41], carbocistein [13, 15], hesperidin [2], and daidzein [16], which decrease $[Cl^-]_i$, enhance CBD leading to increase the rate of mucociliary clearance in nasal epithelia of both types of patients.

Acknowledgements The authors thank Osaka medical College for renting out the video-microscope equipped with a high speed camera. Experiments were carried out in Kyoto Prefectural University of Medicine (2018–2019) and in Ritsumeikan University (2019).

Funding This work was supported by JSPS KAKENHI to YM (No. JP18H03182), JSPS KAKENHI to MY (No. JP18K09325), and research funding from Saisei Mirai.

References

1. Afzelius BA (2004) Cilia-related diseases. J Pathol 2004:470–477
2. Angus SP, Edelmann RE, Pennock DG (2001) Targeted gene knockout of inner arm 1 in Tetrahymena thermophila. Eur J Cell Biol 80:486–497
3. Azbell C, Zhang S, Skinner D, Fortenberry J, Sorscher EJ, Woodwortg BA (2010) Hesperidin stimulates CFTR-mediated chloride secretion and ciliary beat frequency in sinonasal epithelium. Otolaryngol Head Neck Surg 143:397–404. https://doi.org/10.1016/j.otohns.2010.05.021
4. Brokaw CJ (1994) Control of flagellar bending: a new agenda based on dynein diversity. Cell Motil Cytoskeleton 28:199–204
5. Brokaw CJ, Kamiya R (1987) Bending patterns of Chlamydomonas flagella: IV. Mutants with defects in inner and outer dynein arms indicate differences in dynein arm function. Cell Motil Cytoskeleton 8:68–75
6. Chen JC, Lo YF, Lin YW, Lin SH, Huang CL, Cheng CJ (2019) WNK4 kinase is a physiological intracellular chloride sensor. Proc Natl Acad Sci U S A 116:4502–4507
7. Chilvers MA, Rutman A, O'Callaghan C (2003) Ciliary beat pattern is associated with specific ultrastructural defects in primary ciliary dyskinesia. J Allergy Clin Immunol 112:518–524
8. Delmotte P, Sanderson MJ (2006) Ciliary beat frequency is maintained at a maximal rate in the small airways of mouse lung slices. Am J Respir Cell Mol Biol 35:110–117
9. Gibbons IR, Rowe AJ (1965) Dynein: a protein with adenosine triohosphatase activity from cilia. Science 149:424–426
10. Higashijima T, Ferguson KM, Sternweis PC (1987) Regulation of hormone-sensitive GTP-dependent regulatory proteins by chloride. J Biol Chem 262:3597–3602
11. Hirosue S, Senn K, Clement N, Nonnenmacher M, Gigout L, Linden RM, Weber T (2007) Effect of inhibition of dynein function and microtubule-altering drugs on AAV2 transduction. Virology 367:10–18
12. Hosogi S, Miyazaki H, Nakajima K, Ashihara E, Niisato N, Kusuzaki K, Marunaka Y (2012) An inhibitor of Na^+/H^+ exchanger (NHE), ethyl-isopropyl amiloride (EIPA), diminishes proliferation of MKN28 human gastric cancer cells by decreasing the cytosolic Cl^- concentration via DIDS-sensitive pathways. Cell Physiol Biochem 30:1241–1253
13. Ikeuchi Y, Kogiso H, Tanaka S, Hosogi S, Nakahari T, Marunaka Y (2017) Carbocistein-activated bronchiolar ciliary beating via Cl^- and pH-mediated pathways in mice. J Physiol Sci 67(Suppl):S137
14. Ikeuchi Y, Kogiso H, Hosogi S, Tanaka S, Shimamoto C, Inui T, Nakahari T, Marunaka Y (2018) Measurement of $[Cl^-]_i$ unaffected by the cell volume change using MQAE-based two-photon microscopy in airway ciliary cells of mice. J Physiol Sci 68:191–199
15. Ikeuchi Y, Kogiso H, Hosogi S, Tanaka S, Shimamoto C, Matsumura H, Inui T, Nakahari T, Marunaka Y (2018) Carbocisteine stimulated an increase in ciliary bend angle via a decrease in $[Cl^-]_i$ in mouse airway cilia. Pflugers Arch - Eur J Physiol 471:365–380. https://doi.org/10.1007/s00424-018-2212-2
16. Inui T, Yasuda M, Hirano S, Ikeuchi Y, Kogiso H, Inui T, Marunaka Y, Nakahari T (2018) Daizein-stimulated increase in the ciliary beating amplitude via $[Cl^-]_i$ decrease in ciliated human nasal epithelia; cells. Int J Mol Sci 19:3757. https://doi.org/10.3390/ijms19123754
17. Kogiso H, Hosogi S, Ikeuchi Y, Tanaka S, Shimamoto C, Matsumura H, Nakano T, Sano K, Inui T, Marunaka Y, Nakahari T (2017) A low $[Ca^{2+}]_i$-induced enhancement of cAMP-activated ciliary beating by PDE1A inhibition in mouse airway cilia. Pflugers Arch - Eur J Physiol 469:1215–1227
18. Kogiso H, Hosogi S, Ikeuchi Y, Tanaka S, Inui T, Marunaka Y, Nakahari T (2018a) $[Ca^{2+}]_i$ modulation of cAMP-stimulated ciliary beat frequency via PDE1 in airway ciliary cells of mice. Exp Physiol 103:381–390
19. Kogiso H, Ikeuchi Y, Sumiya M, Hosogi S, Tanaka S, Shimamoto C, Inui T, Marunaka Y, Nakahari T (2018b) Seihai-to (TJ-90)-induced activation of airway ciliary beatings of mice: Ca_{2+} modulation of cAMP-stimulated ciliary beatings via PDE1. Int J Mol Sci 19(3):658. https://doi.org/10.3390/ijms19030658
20. Komatani-Tamiya, N, Daikoku E, Takemura Y, Shimamoto C, Nakano T, Iwasaki Y, Kohda Y, Matsumura H, Marunaka Y, Nakahari T (2012) Procaterol-stimulated increases in ciliary bend amplitude and ciliary beat frequency in mouse bronchioles. Cell Physiol Biochem 2012 29: 511–522
21. Kuremoto T, Kogiso H, Yasuda M, Inui T, Murakami K, Hirano S, Ikeuchi Y, Hosogi S, Inui T, Marunaka Y, Nakahari T (2018) Spontaneous oscillation of the ciliary beat frequency regulated by release of Ca^{2+} from intracellular stores in mouse nasal epithelia. Biochem Biophys Res Commun 507:211–216
22. Lorenzo IM, Liedtke W, Sanderson MJ, Valverde MA (2008) TRPV4 channel participates in receptor-operated calcium entry and ciliary beat frequency regulation in mouse airway epithelial cells. Pro Natl Acad Sci USA 105:12611–12616
23. Miertzschke M, Koerner C, Spoerner M, Wittinghofer A (2014) Structural insights into the small G-protein Arl13B and implications for Joubert syndrome. Biochem J 457:301–311
24. Müller L, Brighton LE, Carson JL, Fischer WA, Jaspers I (2013) Culturing of human nasal epithelial cells at the air liquid interface. J Vis Exp 80:e50646. https://doi.org/10.3791/50646
25. Neesen J, Kirschner R, Ochs M, Schmiedl A, Habermann B, Muellwe C, Holstein AF, Nuesslein T, Adham I, Engel W (2001) Disruption on an inner arm dynein heavy chain gene results in asthenozoospermia and reduced ciliary beat frequency. Hum Mol Genet 10:1117–1128
26. Nakajima K, Niisato N, Marunaka Y (2012) Enhancement of tubulin polymerization by Cl^--induced blockade of intrinsic GTPase. Biochem Biophys Res Commun 425:225–229
27. Nakajima K, Marunaka Y (2016) Intracellular chloride ion concentration in differentiating neuronal cell and its role in growing neurite. Biochem Biophys Res Commun 479:338–342

28. Salathe M (2007) Regulation of mammalian ciliary beating. Annu Rev Physiol 69:401–422
29. Shpetner HS, Paschal BM, Vallee RB (1988) Characterization of the microtubule-activated ATPase of brain cytoplasmic dynein (MAP 1C). J Cell Biol 107:1001–1009
30. Shiima-Kinoshita C, Min K-Y, Hanafusa T, Mori H, Nakahari T (2004) β_2-adrenergic regulation of ciliary beat frequency in rat bronchiolar epithelium: potentiation by isosmotic cell shrinkage. J Physiol 554:403–416
31. Shimamoto C, Umegaki E, Katsu K, Kato M, Fijiwara S, Kubota T, Nakahari T (2007) $[Cl^-]_i$ modulation of Ca^{2+}-regulated exocytosis in ACh-stimulated antral mucous cells of Guinea pig. Am J Physiol Gastrointest Liver Physiol 293:G824–G837
32. Sutto Z, Conner GE, Salathe M (2004) Regulation of human airway ciliary beat frequency by intracellular pH. J Physiol 560:519–532
33. Terker AS, Zhang C, Erspamer KJ, Gamba G, Yang CL, Ellison DH (2016) Unique chloride-sensing properties of WNK4 permit the distal nephron to modulate potassium homeostasis. Kidney Int 89: 127–134
34. Tohda H, Foskett JK, O'Brodovich H, Marunaka Y (1994) Cl^- regulation of a Ca^{2+}-activated nonselective cation channel in beta-agonist-treated fetal distal lung epithelium. Am J Phys Cell Phys 266:C104–C109
35. Tokuda S, Shimamoto C, Yoshida H, Murao H, Kishima G, Ito S, Kubota T, Hanafusa T, Sugimoto T, Niisato N, Marunaka Y, Nakahari T (2007) HCO_3^--dependent pH_i recovery and overacidification induced by NH_4^+ pulse in rat lung alveolar type II cells: HCO_3^--dependent NH_3 excretion from lungs? Pflugers Arch - Eur J Physiol 455:223–239
36. Treharne KJ, Marshall LJ, Mehta A. A novel chloride-dependent GTP-utilizing protein kinase in plasma membranes from human respiratory epithelium. Am J Physiol 267 (Lung Cell Mol Physiol 11) 267: L592-L601, 1994
37. Wanner A, Salathe M, O'Riordan TG (1996) Mucociliary clearance in the airways. Am J Respir Crit Care Med 154:1868–1902
38. Wood CR, Hard R, Hennessey TM (2007) Targeted gene disruption of dynein heavy chain 7 of Tetrahymena thermophila results in altred ciliary waveform and reduced swim speed. J Cell Sci 120: 3075–3085
39. Yaghi A, Dolovich MB (2016) Airway epithelial cell cilia and obstructive lung disease. Cells 5(4):40. https://doi.org/10.3390/cells5040040
40. Yasuda M, Niisato N, Miyazaki H, Iwasaki Y, Hama T, Dejima K, Hisa Y, Marunaka Y (2007) Epithelial Na^+ channel and ion transport in human nasal polyp and paranasal sinus mucosa. Biochem Biophys Res Commun 362:753–758
41. Yasuda M, Niisato N, Miyazaki H, Hama T, Dejima K, Hisa Y, Marunaka Y (2007) Epithelial ion transport of human nasal polyp and paranasal sinus mucosa. Am J Respir Cell Mol Biol 36:466–472
42. Zhang L, Sanderson MJ (2003) The role of cGMP in regulation of rabbit airway ciliary beat frequency. J Physiol 551:765–776